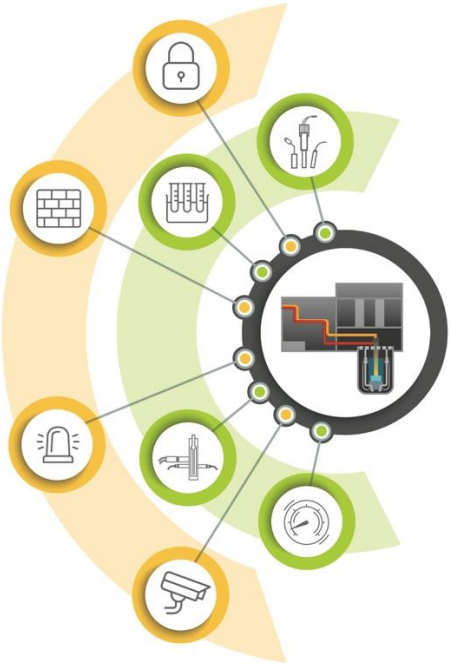

On-line Monitoring for Molten Salt Reactor MC&A: Optical Spectroscopy-Based Approaches

Prepared for
US Department of Energy

**A.M. Lines, S.A. Bryan,
H.M. Felmy, and S.D. Branch**

Pacific Northwest National Laboratory

**September 2021
PNNL-31955**

SUMMARY

Molten salt reactors (MSRs) represent a key green energy technology that can meet changing world energy demands. Within the United States, support and interest for these reactor designs can be observed, including examples of DOE support through the Advanced Reactor Deployment Program and GAIN. Significant technological progress is being made with MSR reactor design, but questions still remain in how material control and accounting (MC&A) approaches can be translated or created for MSR processes.

The MSR environment is challenging to monitor. High temperatures, corrosive salts, and radiation all complicate monitoring and sample collection and analysis. The integration of process monitoring, where *in situ* sensors can limit the need to collect grab samples, can be an ideal opportunity for MSRs. The primary goal of this work is to evaluate the applicability of on-line optical approaches to maintaining MC&A of molten salt systems.

This report focuses on U as a demonstration species, with the intent of capturing U fingerprints under a variety of salt conditions in multiple oxidation states. This focused on simple systems (i.e., lacking interfering corrosion or fission product simulants) with the goal of expanding to these more complex chemical systems in subsequent fiscal years. Ultraviolet-visible (UV-vis) and Raman spectroscopic analyses were utilized to measure uranium chloride salts in LiCl-KCl and NaCl-KCl-$MgCl_2$ eutectics.

The setup and methodology for performing molten salt spectroscopic measurements is presented. A preexisting small-scale setup was utilized for optical data collection. The general system design has been used by the PNNL team previously, while the system used here includes specific modifications to furnace materials and optical probe integration to allow for air-sensitive measurements. A significant aspect of the modifications includes transitioning the heater and optical components into an inert glove box. This enables the interrogation of molten salts under controlled atmospheric conditions more closely approximating those of an MSR. The glovebox is maintained under Ar atmosphere with reduced levels of O_2 and moisture. The custom furnace for handling molten samples sits inside of the glovebox, with several feedthroughs installed to accommodate connection to spectroscopic, temperature, and potentiostat instruments housed outside of the glovebox.

The ability to spectroscopically measure various oxidation states of uranium was demonstrated for U(IV) and U(VI) within the NaCl-KCl-$MgCl_2$ eutectic. This was performed by the sequential addition of U(IV) in the chemical form UCl_4 into dual UV-vis/Raman spectroscopic cell while measuring the spectroscopic signatures of the solution species. The UV-vis and Raman spectroscopic methods followed the chemical conversion of U(IV) to U(VI) during the heating period of this experiment. The quantitative conversion of the U(IV) to U(VI) was confirmed by the on-line monitoring and partial least-squares modeling of the solution phase. The extinction coefficients for both U(IV) and U(VI) were confirmed to be consistent with literature for the UV-vis spectra of these species. In addition, the limits of detection for U(IV) and U(VI) were determined for these techniques. Similarly, the fingerprints of U(III), U(IV), and U(VI) were characterized within a LiCl-KCl eutectic. Finally, some initial demonstrations of chemometric modeling were completed. Overall, results are positive and lay the necessary foundation to make final recommendations regarding optical MC&A approaches in the upcoming fiscal year.

CONTENTS

FIGURES

TABLES

ACRONYMS AND ABBREVIATIONS

CV	cyclic voltammogram
DOE	US Department of Energy
FY	fiscal year
LOD	limit of detection
MC&A	material control and accounting
MSR	molten salt reactor
PLS	partial least-squares
PNNL	Pacific Northwest National Laboratory
UV-vis	ultra-violet visible spectroscopy

1. INTRODUCTION

Molten salt reactors (MSRs) are gaining interest internationally as a next-generation reactor design that can safely and efficiently meet green energy needs. Within the United States, support and interest for these reactor designs can be seen in the awarding of Advanced Reactor Deployment Program funding to Terra Power and Southern Company for their proposed MSR technology in 2020. While various organizations are making excellent progress in addressing the technological and regulatory questions regarding MSRs, questions still remain in how material control and accounting (MC&A) approaches can be translated or created for MSR processes.

The complexities of the MSR environment, high temperatures and radiation combined with highly corrosive streams, are made more challenging by the need to keep the molten salt in a closed and inert atmosphere. This is an ideal opportunity to integrate in-line monitoring, where *in situ* sensors can limit the need to open atmospheric-controlled systems to collect grab samples.

Several technologies can be adapted to the molten salt environment, with one key option being optical spectroscopy (Polovov et al. 2008; Park et al. 2011; Nagai et al. 2013; Schroll et al. 2013; Schroll et al. 2016a; Schroll et al. 2016b; Schroll et al. 2017). This approach can provide unique insights into speciation and oxidation states, which can be highly valuable in accurately accounting for actinides that display complex chemistry under molten salt conditions. Previous demonstrations indicate optical monitoring approaches can be combined with advanced analysis techniques including chemometric modeling for the real-time analysis of complex chemical process streams including Hanford waste and used nuclear fuel reprocessing schemes (Bryan et al. 2011; Lines et al. 2018; Lines et al. 2019; Lines et al. 2020a; Lines et al. 2020b; Tse et al. 2020). Transitioning these technologies to molten salt systems requires key technology advances, which were identified and outlined in a previous report (Paviet et al. 2020), with Figure 1-1 below outlining the key areas. This roadmap and the previous report summarize target analytes and technology needed to monitor species and serves as a technology development roadmap. For safeguard concerns, the initial metals considered for MC&A purposes included U (Nagai et al. 2013), Pu (Shirai et al. 1998; Serp et al. 2004; Bourgès et al. 2007), and Np (Polovov et al. 2007).

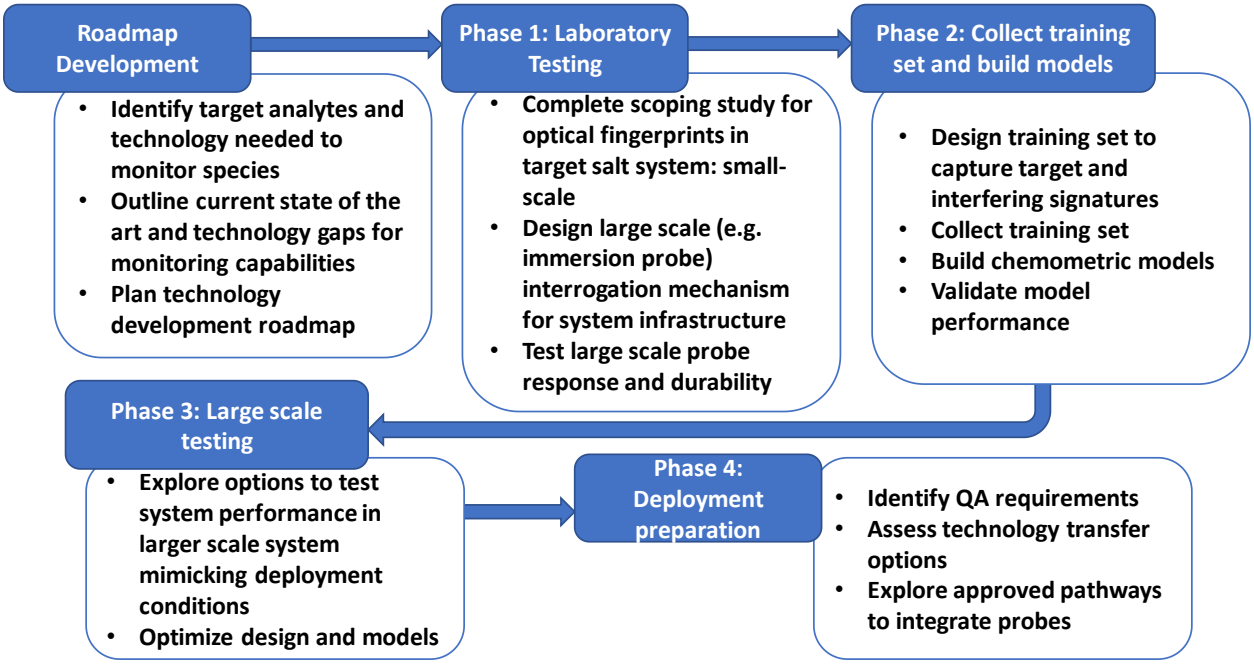

Figure 1-1. Roadmap for on-line monitoring technology development (Paviet et al. 2020).

Project work in fiscal year (FY) 2021 was focused on building an optical library of uranium fingerprints within molten salt systems. While this generally focused on simplistic systems (lacking interfering species as anticipated in real fuel melts), optical characteristics presented significant dependence on salt impurities and, by association, salt cleaning methods. However, optical-based approaches can provide insights into these complexities that can potentially impact accurate analysis for U via other on-line or off-line characterization approaches. Overall, optical approaches can be successfully applied to molten salt systems, but further effort is needed to build an optical library that captures the variability of optical fingerprints as a function of salt conditions and the presence of interferents. The following sections outline FY21 progress and provide insight into FY22 opportunities.

2. SETUP AND METHODOLOGIES

Characterization of molten salt systems can be challenging due to the corrosivity of the melt, the high temperatures of the system, and the need to maintain an inert environment. The sections below discuss the system setup to enable representative on-line interrogation of the salt. Note that FY21 work focused on small-scale system demonstrations to enable more efficient and cost-effective evaluation of optical approaches. These approaches are translatable to larger-scale designs.

2.1 Small-Scale Molten Salt Setup

A preexisting small-scale setup was utilized for optical data collection. The general system design has been described previously (Schroll et al. 2013; Schroll et al. 2016b; Schroll et al. 2017) while the system used here included some modifications to furnace materials and optical probe integration. Figure 2-1 below presents a schematic of the small-scale system. It also includes schematics showing the electrode setup. This system relies on spectroelectrochemical approaches to enable control of oxidation states of target species within the salt melt. In this case, the system was utilized to modulate U between the 4+ and 3+ oxidation states.

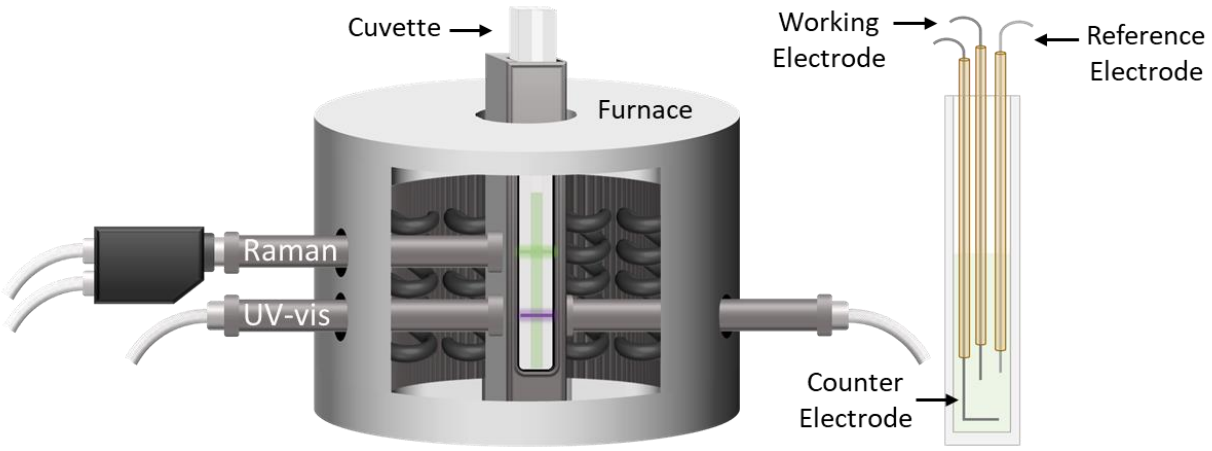

Figure 2-1. Schematic of the small-scale setup showing the clam-shell furnace containing the cuvette holder with optics for Raman and UV-vis measurements which are connected to the instruments via fiber optic cables. The electrode configuration is shown within the cuvette containing the molten salt.

Electrode setups focused the use of Pt or W working and counter electrodes. Data presented in the Results and Discussion section will include details where appropriate.

Instruments utilized included Raman and UV-vis spectroscopic systems acquired from Spectra Solutions Inc. with thermoelectric-cooled charge-coupled device detectors. The Raman system included a 532 nm (220 mW) diode laser with approximately 400-4200 cm^{-1} spectral range and ~2 cm^{-1} resolution. The UV-vis system had a functional spectral range of 450-850 nm. The potentiostat utilized was a Reference 3000 (Gamry Instruments Inc., Warminster, PA) operated using Framework™ data acquisition software (v7.8.2).

2.2 Completing Inert Box Setup

A significant aspect of FY21 work was transitioning the setup to an inert glove box. This enables the interrogation of molten salts under controlled atmospheric conditions more closely approximating those of an MSR. The glovebox is maintained under Ar atmosphere O_2 <0.4 ppm and moisture <5 ppm. Internal box pressure is maintained at 1.0 – 2.2 mbar. The custom furnace for handling molten samples sits inside

of the glovebox, with several feedthroughs installed to accommodate connection to spectroscopic, temperature, and potentiostat instruments housed outside of the glovebox. Sample equipment (e.g. cuvettes, electrodes, etc.) are thoroughly cleaned and heated at ≥150°C to remove contaminants before being placed in the glovebox.

2.3 Salt Conditions

Although the salts for this work were purchased at the highest purities commercially available (99.99 – 99.999%), several literature sources indicate additional cleaning of the salts is required as they contain reactive impurities, such as moisture and hydroxides. Maintaining high-purity salts, even at the small scale (<1 mL molten solution) is a challenge. To gain a better understanding of the impacts of these impurities in molten salts, a majority of FY21 efforts was conducted using commercially available salts without further purification, to serve as a model for purities at the MSR scale. In addition, an experiment was conducted to compare the optical fingerprints of U in cleaned LiCl-KCl salt. A summary of this cleaning process is discussed in Section 3.2.2.

Uranium (IV) chloride (99.99%) was purchased from Bio-Analytical Industries, Inc. (Doyline, LA) and used without further purification. This source of U was prepared using dichlorination of uranium oxide with hexa-chloropropene. Uranium (III) chloride was acquired from TerraPower and used without further purification.

3. RESULTS AND DISCUSSION

The primary goal of FY21 work was to evaluate the applicability of on-line optical approaches to maintaining MC&A of molten salt systems. To achieve this, the team focused on U as a demonstration species, with the intent of capturing U fingerprints under a variety of salt conditions in multiple oxidation states. This generally focused on simple systems (i.e., lacking interfering corrosion or fission product simulants) with the goal of expanding these to more complex chemical systems in subsequent fiscal years.

3.1 Calibration Curves and Limits of Detection for Uranium

The U chemical targets include U(III) and U(IV). Most MSR vendors plan on limiting U speciation to these two oxidation states and maintaining a balanced ratio of U(III) to U(IV) that limits corrosion. Typically, this means pursuing ratios low in U(IV) and high in U(III). This presents a challenge for UV-vis absorbance quantification approaches. Literature shows U(IV) exhibits a substantially lower molar absorptivity as compared to U(III) (Polovov et al. 2008; Nagai et al. 2013). Lower concentrations of U(IV) mean larger pathlengths will likely be needed to quantify target species; however, higher concentrations of U(III) mean shorter pathlengths are needed to avoid saturating the detector. This will be true in both chloride and fluoride-based salt systems. Fortunately, achieving needed pathlengths is a relatively straightforward engineering challenge. It requires building initial calibration curves to determine needed pathlengths for each system to best characterize working ranges of U targets. If dual probes are needed, one for each oxidation state, this can be accomplished by introducing two probes that can be run on the same instrument/data analysis system. Analysis to quantify one oxidation state in the presence of the other is also a challenge but will be discussed in a later section.

To explore the detectable range of U in molten salts, initial single-variate calibration curves were generated and used to calculate limits of detection (LODs) for target species. Note, impacts of salt purity and presence of interfering analytes can be significant and will be discussed in later sections.

Because U(IV) is anticipated to be the more difficult species to quantify, it was the initial focus of quantification efforts. Multiple salt systems were explored, including LiCl-KCl and NaCl-KCl-$MgCl_2$ eutectics. Different salt systems exhibit different challenges such as high melting points, therefore, the relatively low melting points of ~350°C for LiCl-KCl and ~400°C for NaCl-KCl-$MgCl_2$ (Clark 1965), made these salt systems logical first choices. In initial testing, the NaCl-KCl-$MgCl_2$ eutectic generally performed well and calibration curve data for U(IV) could be effectively generated and captured. Figure 3-1 below presents examples of the spectral fingerprints and the resulting calibration curve.

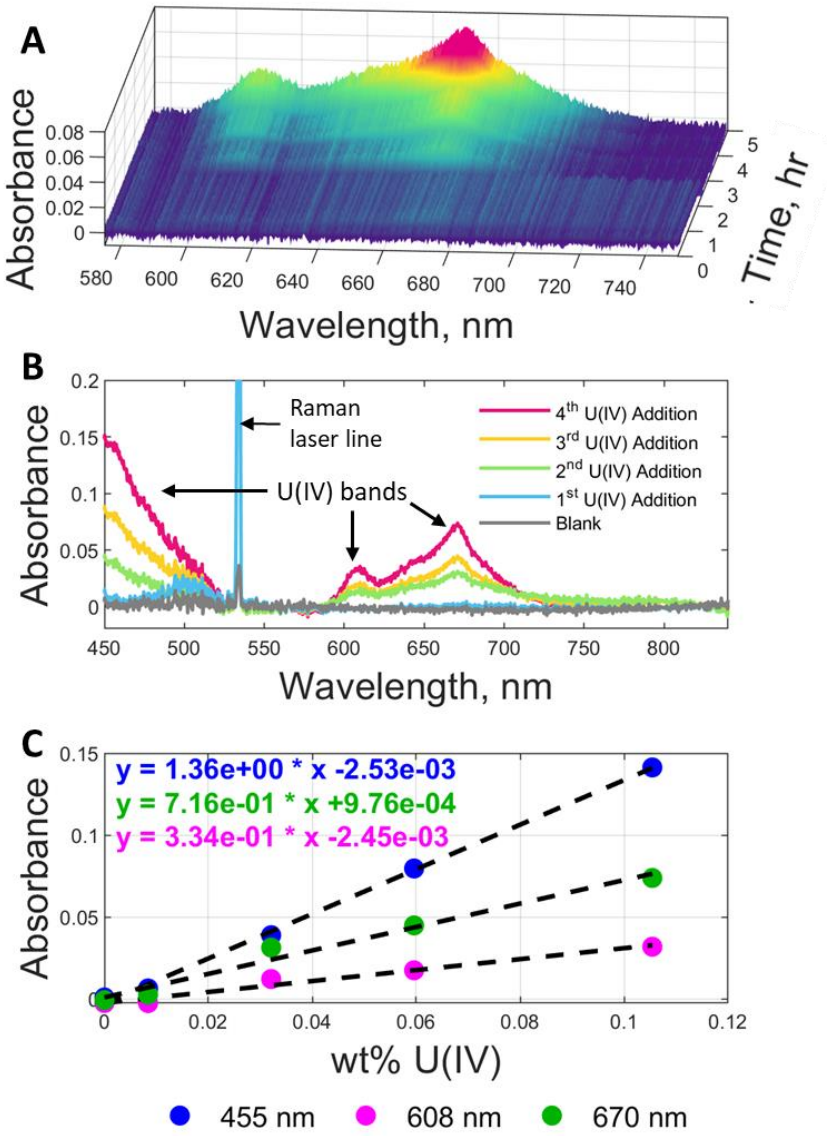

Figure 3-1. U(IV) in NaCl-KCl-$MgCl_2$ eutectic at 600°C showing (a) the UV-vis absorbance spectra with successive additions of UCl_4 highlighting the main U(IV) absorbance bands, (b) an average of 100 spectra after each addition showing the full absorbance range, and (c) calibration curves for each U(IV) band with the resulting wt% LOD. The integration time was 3 sec, the path length was 2 mm and the spectra were referenced to the molten blank NaCl-KCl-$MgCl_2$ salt before the addition of U(IV). The spectra were baseline corrected.

The calibration curves shown in Figure 3-1c were used to calculate the limit of detection for each major U(IV) band under those conditions reported here:

$$\text{LOD} = \frac{3s}{m} \qquad \text{EQN 3-1}$$

where, *s* is the noise of the blank measured at each wavelength and *m* is the slope of the calibration curve (Harris 2007). The molar absorptivities and LODs were calculated for each of the major U(IV) bands (approximately 455, 608, and 670 nm) and are shown in Table 3-1. The best limit of detection was 0.27 wt% (18 mM) U(IV) using the band at 670 nm. The U(IV) optical fingerprint and molar absorptivities were

similar to past literature of different salt systems demonstrating that the salt composition does not have a major impact on the optical fingerprints (Nagai et al. 2005).

Also observed in this study was the conversion of U(IV) to U(VI) while the salt was allowed to sit overnight. Figure 3-2 shows the UV-vis fingerprint of U(VI) with the calculated molar absorptivity at 455 nm of 60.2 $L \cdot mol^{-1} \cdot cm^{-1}$. The optical fingerprint and molar absorptivity were in good agreement with literature (Nagai et al. 2004), giving strong support that the U was present as the U(VI) uranyl ion (i.e., UO_2^{2+}). The further discussion of this oxidation state change is presented in Section 3.2.

It is important to note that the band at 455 nm will overlap with the absorbance fingerprint of U(VI), but there is very little overlap with the U(IV) bands at 608 and 670 nm so these bands can still be used to track the presence of U(IV) when U(VI) is present.

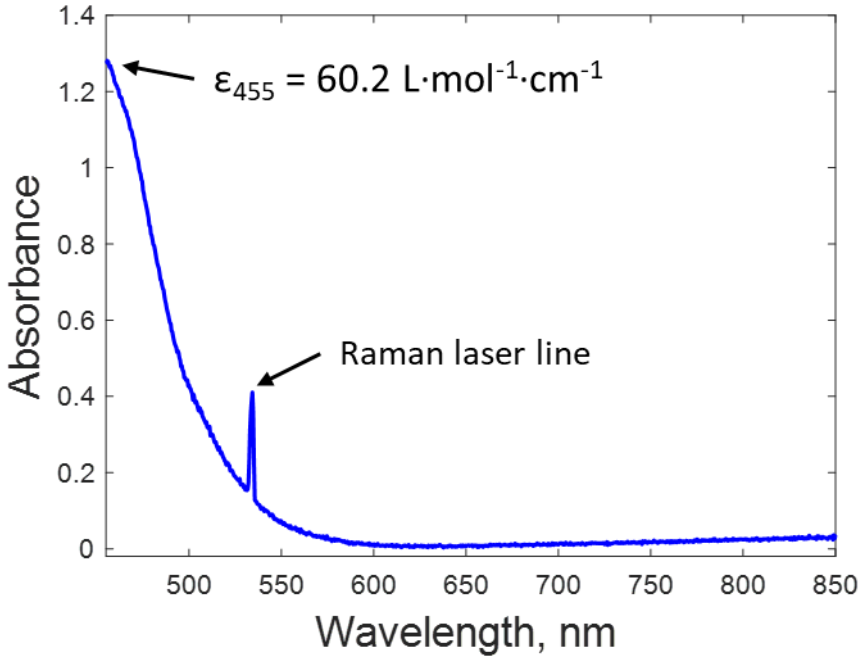

Figure 3-2. U(VI) UV-vis spectrum in NaCl-KCl-$MgCl_2$ eutectic at 600°C. The band at 532 nm is a result of the Raman laser. The integration time was 3 sec and the spectrum represents an average of 100 spectra.

3.2 Impacts of Impurities and Interferents

In on-line monitoring applications, the presence and impact of interferents should be anticipated and mitigation strategies should be built into quantification algorithms. The PNNL team has significant experience with this and can leverage these approaches when building tool kits for molten salt systems. Overall, this involves chemometric modeling of optical data. These machine learning tools utilize multivariate algorithms to translate complex optical data into information such as concentration and ratios.

However, it is important to note that in the case of molten salt systems, interferents can fit into two primary categories:

1) Spectral fingerprint overlaps or interferes with target fingerprint(s)
2) Solution interferent chemically interacts with target species and changes target speciation and fingerprint(s)

Methods to overcome these separate challenges are needed. The current state of the art, and examples of needed next steps are described below in more detail.

Optical fingerprint overlap

Fingerprint overlap is by far the easier challenge to overcome. This has been demonstrated for complex salt melts containing multiple lanthanides (Schroll et al. 2016b), as well as on non-molten salt media exhibiting even more complex optical interferences (Lines et al. 2017; Lines et al. 2018; Nelson et al. 2018; Lines et al. 2019; Lines et al. 2020b). The solution to this challenge lies in chemometric modeling of the system. This machine learning approach leverages multivariate analysis and enables robust characterization in the face of complex data. Overall, chemometric modeling approaches previously developed and demonstrated can be translated to molten salt data analysis when building quantification algorithms for those systems.

Chemical interactions impacting target speciation and fingerprint

Complex chemistry impacting optical fingerprints is a more significant challenge. Methods for building models that can be robust and accurate in the face of changing speciation have been demonstrated (Lines et al. 2017; Nelson et al. 2021). However, the success of these models was predicated on building training sets that captured the unique fingerprints of the different species. This can be challenging to accomplish if the chemistry or the speciation of the chemical system is not well understood. Within molten salt systems, limited literature makes this challenging. Some chemical targets, such as U, do have a good foundation in literature but most studies are completed in very pure salt systems with active chemical redox control, leaving open questions on behavior in more complex melts. A better basis is needed for understanding U chemistry where optical monitoring probes can play a key role. Examples of this challenge and the role of optical spectroscopy are provided in the following sections.

3.2.1 Uranium Speciation Impacts Within NaCl-KCl-$MgCl_2$ Eutectic Containing Minor Impurities

Note, this system was explored using 99.999% NaCl and KCl and 99.99% $MgCl_2$. While several publications utilize salts at these purity levels for their studies, results from work here indicate even the small amounts of impurities present can significantly impact U speciation and fingerprints without some form of redox control; Figure 3-3 and Figure 3-6 below presents a clear demonstration of this. Spectral response over time is presented through the course of a single experiment. In this system a blank salt was first melted, then UCl_4 was added in a series of 4 pucks and allowed to dissolve. The system was then allowed to sit overnight at which point U(IV) began converting to U(VI) in the form of the uranyl ion. The following morning, the 5th and 6th additions of UCl_4 were introduced to the system. After the 6th addition of UCl_4, the electrodes were added to the cuvette and allowed to sit before any electrochemistry was performed. This point is labeled “E” in the bottom plot of Figure 3-3(b). At the point when the electrodes were added to the system, there was an observed conversion of the U(VI) to U(IV) shown by a drop in the 455 nm peak and growth of the 670 nm U(IV) band. Figure 3-6 shows the Raman spectra collected during the same experiment and shows an increase in the 842 cm^{-1} uranyl band (Polovov et al. 2008) during the time when the system was allowed to sit overnight and a decrease in this band with further additions of UCl_4 and after the addition of the electrodes.

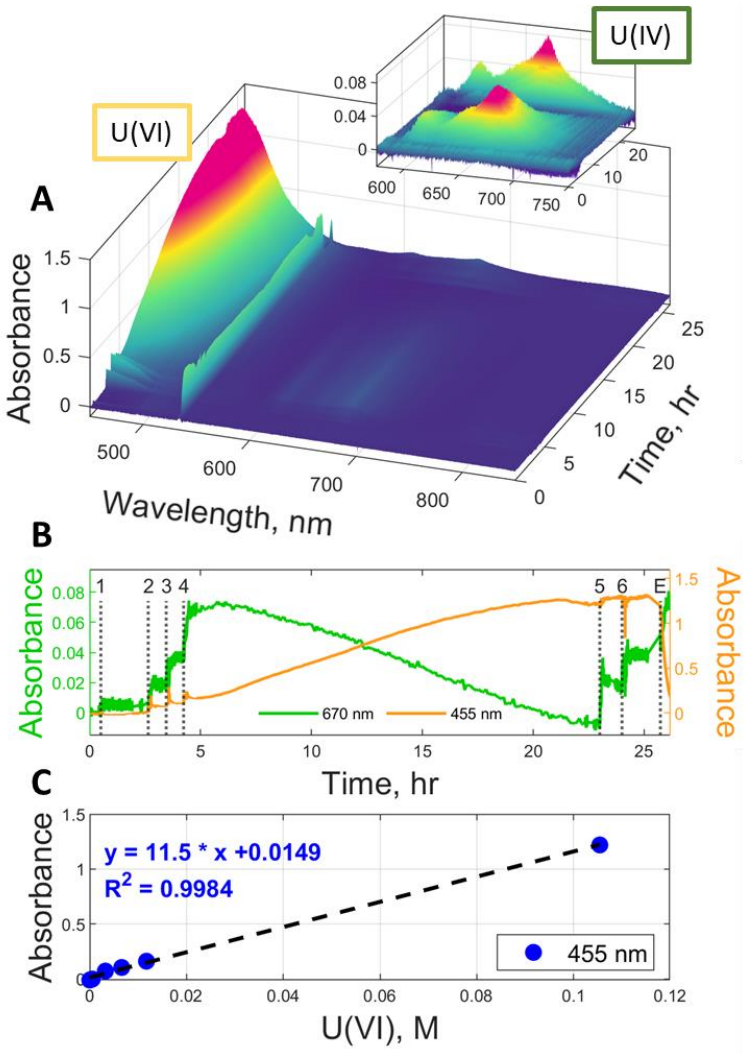

Figure 3-3. U behavior in the NaCl-KCl-$MgCl_2$ eutectic at 600°C over time showing the (a) UV-vis spectra over the course of the ~26 hr experiment with an inset showing the primary U(IV) bands in the 600-750 nm range, (b) the measured absorbance at the 670 nm peak associated with U(IV) and the 455 nm peak, which is mainly a result of U(VI) absorbance, and (c) the LOD calculation of calibration curve for U(VI) from the conversion of U(IV) to U(VI). The time of each of the 6 additions of U(IV) are labeled in (b) as well as the addition of the electrodes to the cuvette – labeled "E". The integration time was 3 sec.

The uranium speciation observed in Figure 3-3a shows the conversion from U(IV) to U(VI) over the course of ~26 hours. While the trace of the absorbance vs time for the absorbance bands associated with the primary peaks for U(IV) and U(VI) indicate the conversion between the U(IV) starting material to the U(VI) complex over the 26-hour timeframe, this is not a quantitative measure of the conversion. By using the multivariate approach of chemometric analysis, it is possible to determine the concentrations of the uranium species in solution at each time during this experiment.

Using the spectra in Figure 3-1 as the basis for a training set of spectra, it is possible to construct a partial least-squares (PLS) model for the measurement of U(IV) and U(VI). The fit of the models for both U(IV) and U(VI) is shown in Figure 3-4a and Figure 3-4b, showing the fit of the line and R^2 fitting parameters.

In both cases, the slope of the fit of the line is near unity, and the *y*-intercept value is close to zero, showing optimum performance.

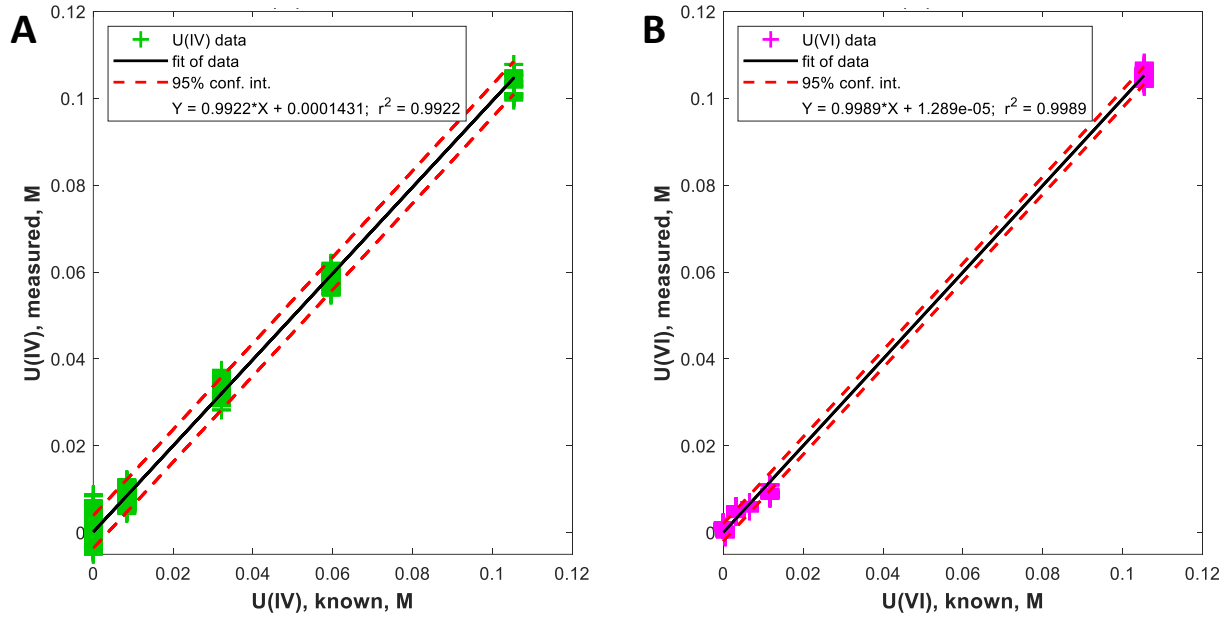

Figure 3-4. PLS models for the measurement of (a) U(IV) and (b) U(VI).

These PLS models were then used to predict the concentrations of U(IV) and U(VI) in the dataset shown in Figure 3-3a. As can be seen from this figure, the incremental addition of U(IV) is apparent for the first four additions (labels 1 through 4, Figure 3-5b). The slow conversion of U(IV) to U(VI) is also observed between hour 5 through ~ 23. After the 23 hr time, two more U(IV) additions were made (labels 5 and 6) where the concentration of U(IV) was observed to increase. At approximately 26 hrs, the electrodes were inserted followed by the chemical reduction of U(VI) to U(IV), based on the measured concentration.

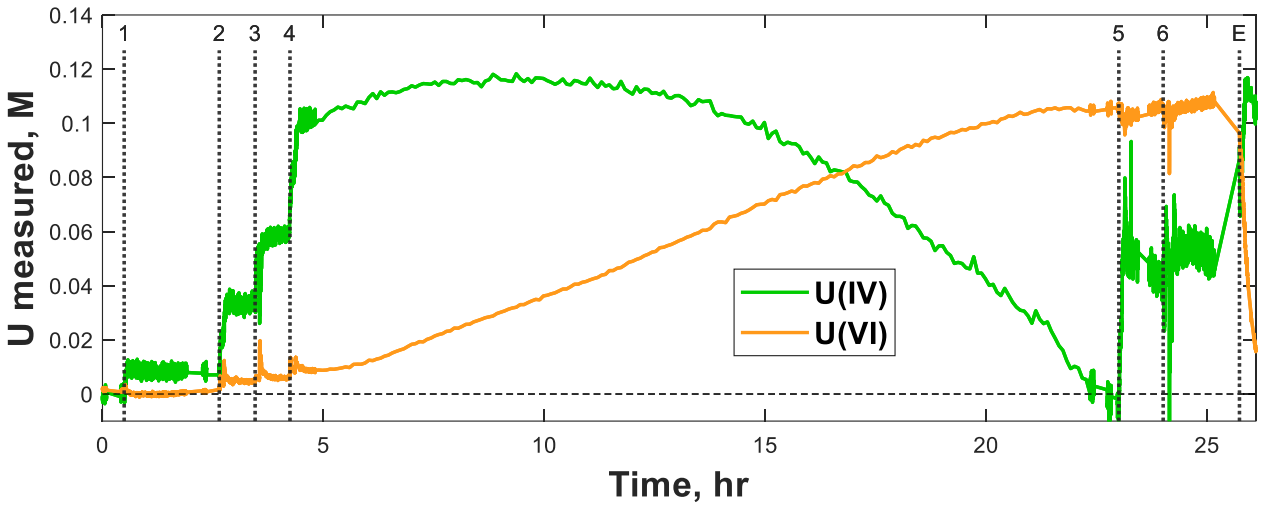

Figure 3-5. Measured U(IV) and U(VI) concentrations in the NaCl-KCl-$MgCl_2$ eutectic at 600°C over 26 hours showing the conversion from U(IV) to U(VI). The labels "1" through "6" indicate the times of U(IV) addition; the label "E" indicated the time electrodes were inserted into the system.

Figure 3-6 shows the Raman spectra collected during the same experiment and shows an increase in the 842 cm^{-1} uranyl band during the time when the system was allowed to sit overnight and a decrease in this band with further additions of UCl_4 and after the addition of the electrodes. Figure 3-7 shows photos taken when the cuvette was removed from the furnace during the experiment. The green U(IV) can be seen in the photo taken after the 4th addition of UCl_4 and the yellow color in the photo taken after the system was allowed to sit overnight is indicative of the conversion to U(VI).

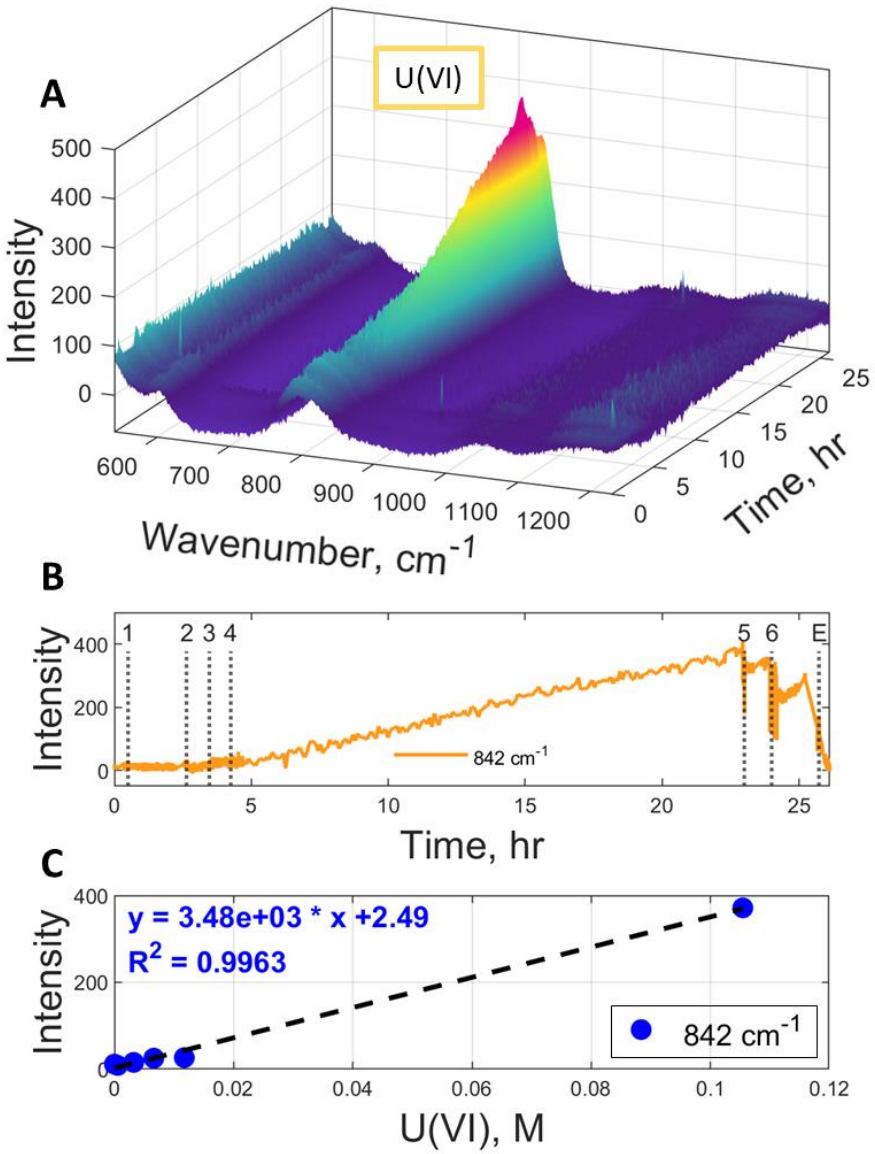

Figure 3-6. U behavior in the NaCl-KCl-$MgCl_2$ eutectic at 600°C over time showing the (a) Raman spectra over the course of the ~26-hour experiment, (b) the measured intensity at the 842 cm^{-1} uranyl peak, and (c) a two-point calibration curve to calculate based on the LOD for U(VI) band intensity. The time of each of the 6 additions of U(IV) are labeled in (b) as well as the addition of electrodes to the cuvette – labeled "E". Each spectrum is an average of 5 spectra. The integration time was 1 sec.

Table 3-1 Weight % and molar concentration LODs along with molar absorptivities (ε) for each of the major U(IV) and U(VI) peaks measured using UV-vis and Raman spectroscopy.

Species	Method	Peak location	LOD, wt%	LOD, M	ε, $L \cdot mol^{-1} \cdot cm^{-1}$
U(IV)	UV-vis	455 nm	0.31	0.021	6.9
U(IV)	UV-vis	608 nm	0.60	0.041	1.5
U(IV)	UV-vis	670 nm	0.27	0.018	3.5
U(VI)	UV-vis	455 nm	0.013	0.0009	60.2
U(VI)	Raman	842 cm^{-1}	0.17	0.012	N/A

Figure 3-7. Photos of U in the NaCl-KCl-$MgCl_2$ eutectic at 600°C taken (a) during the experiment shown in Figure 3-3 and Figure 3-6 after the 4th addition of UCl_4 showing the green U(IV) and (b) after overnight heating before the 5th addition of UCl_4 showing the yellow U(VI).

After the electrodes were added (W wire working and counter electrodes and Ag wire reference) to the solution, the U(VI) began to convert back to the U(IV) even before any electrochemical experiments were

performed to characterize the system. Figure 3-8 shows a series of cyclic voltammograms (CVs) collected on this system. There were several couples evident in the CVs, many of which were also apparent in a previous blank experiment done on the same salt eutectic without U present. This indicates the presence of impurities in the salt.

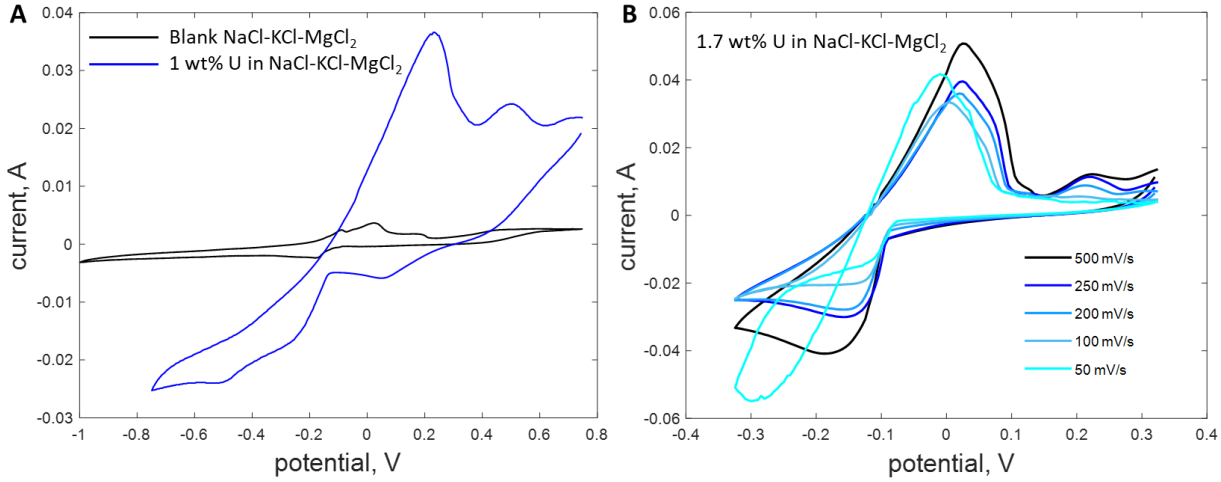

Figure 3-8. Cyclic voltammograms (CVs) of (a) a previous experiment comparing a 1 wt% U salt to a blank salt of the same NaCl-KCl-$MgCl_2$ eutectic and (b) a series of CVs at varying scan rate measured on the same system as the previous plots at 1.7 wt% U added. Electrode configuration: working: W wire, counter: W wire, reference: Ag wire.

In an attempt to electrochemically form U(III), reducing potentials were applied during controlled potential electrolysis experiments. When reducing potentials were applied, however, black dendrites were formed on the working electrode that interfered with both the electrode function and the UV-vis signal. Figure 3-9 shows photos before and after a 3.5-minute, -0.4 V reducing potential was applied to the system. The dendrites are clearly visible around the center working electrode. The salt remained green, which is indicative of U(IV), with no evidence of the formation of red U(III) complex.

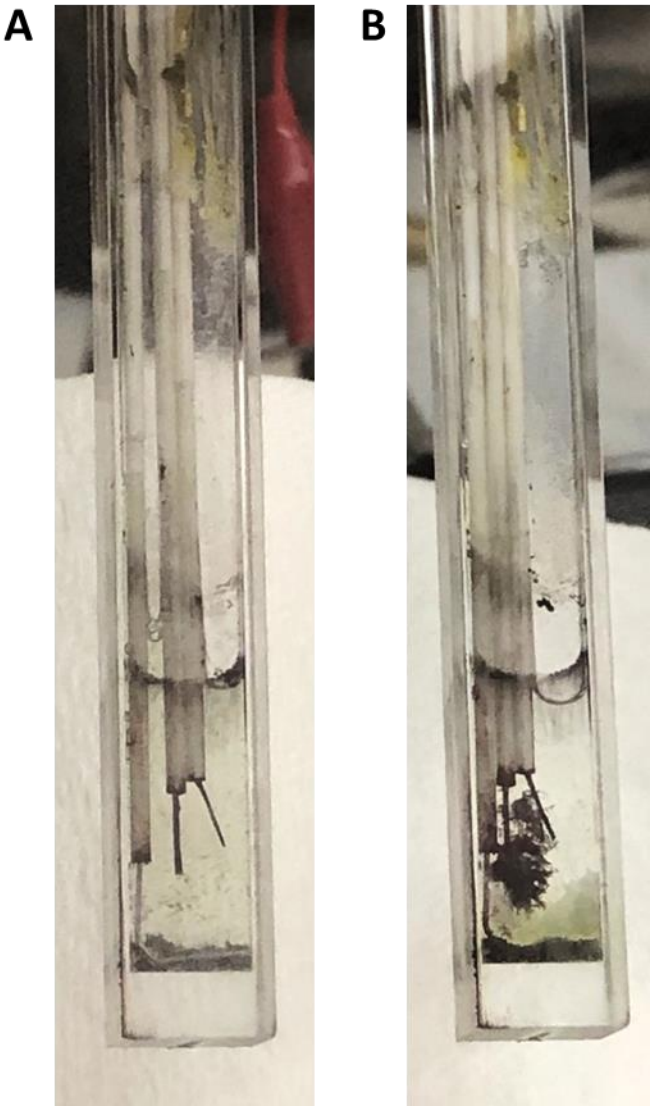

Figure 3-9. Photos of U in the NaCl-KCl-$MgCl_2$ eutectic at 600°C taken following the data shown in Figure 3-3 and Figure 3-6 (a) before and (b) after the application of a -0.4 V reducing potential.

Overall, there are several conclusions from this demonstration. Without some form of monitoring that provides insight into U speciation, it will be very difficult to understand/control U chemistry in a salt melt where fission and corrosion products are continuously being generated. For MC&A purposes, this is not a significant issue unless U or other key species begin to form oxides and precipitate out of solution. In several of the eutectic solutions containing U characterized here, black precipitates were observed that may contain U. Note all these salts were procured as high purity, anhydrous salts and were handled within inert containment. These salts were not cleaned through the chemical means sometimes used by other researchers, including sparging with Cl_2, or through other electrochemical means such as generating sacrificial U metal.

Model accuracy and uncertainty in measurements are directly tied to the accuracy of training sets used to build models. Without precise control of speciation and resulting fingerprints during data collection, uncertainties in quantification may be undesirably high. For the purposes of chemometric model building,

this poses additional challenges. This is true for any monitoring and data analysis approach including for MC&A purposes.

Most important to note in the example here is that while U(IV) and U(VI) (as the uranyl complex) could be fairly well captured and characterized, it was extremely difficult to generate and maintain U(III). Within this system, spectroelectrochemistry was employed to control oxidation states of the targets. Figure 3-8 shows a series of cyclic voltammograms (CVs) of the salt melt characterized in Figure 3-3 and Figure 3-6 above. The CV shows notable complexity but still generally indicates the redox couple for U(III)/U(IV). However, applying potentials to produce U(III) did not result in the ingrowth of the U(III) optical fingerprint. Instead, the generation of black solids that steadily blocked optical windows was observed. This was paired with a decrease in both the U(IV) UV-vis fingerprint and reduction in current from the subsequent CVs of the U(III)/U(IV) couple, indicating U was being lost to the formation of the black solid. Most likely, U(III) was generated but reacted very quickly with salt impurities to form the precipitates. Because of this behavior, it was not possible to collect optical training sets for U(III) within this salt system via electrochemical means.

3.2.2 Looking at Cleaned Salt Systems

The salt purification approach is detailed below. A schematic of the salt cleaning vessel and resulting cleaned salt are shown in Figure 3-10. The following sequential steps were used in the salt cleaning process.

- Heat crucible in reactor at 650°C with dynamic pumping overnight to remove moisture.
- Add salt to crucible in reactor.
- Heat in incremental steps to 350°C with dynamic pumping to remove moisture from salt at each step.
- Heat incrementally to 550°C with dynamic pumping to melt salt.
- Sparge molten salt with HCl at 550°C for 6 hr.
- Bring salt back to room temperature with dynamic pumping.
- Open reactor in inert box to remove salt from crucible.

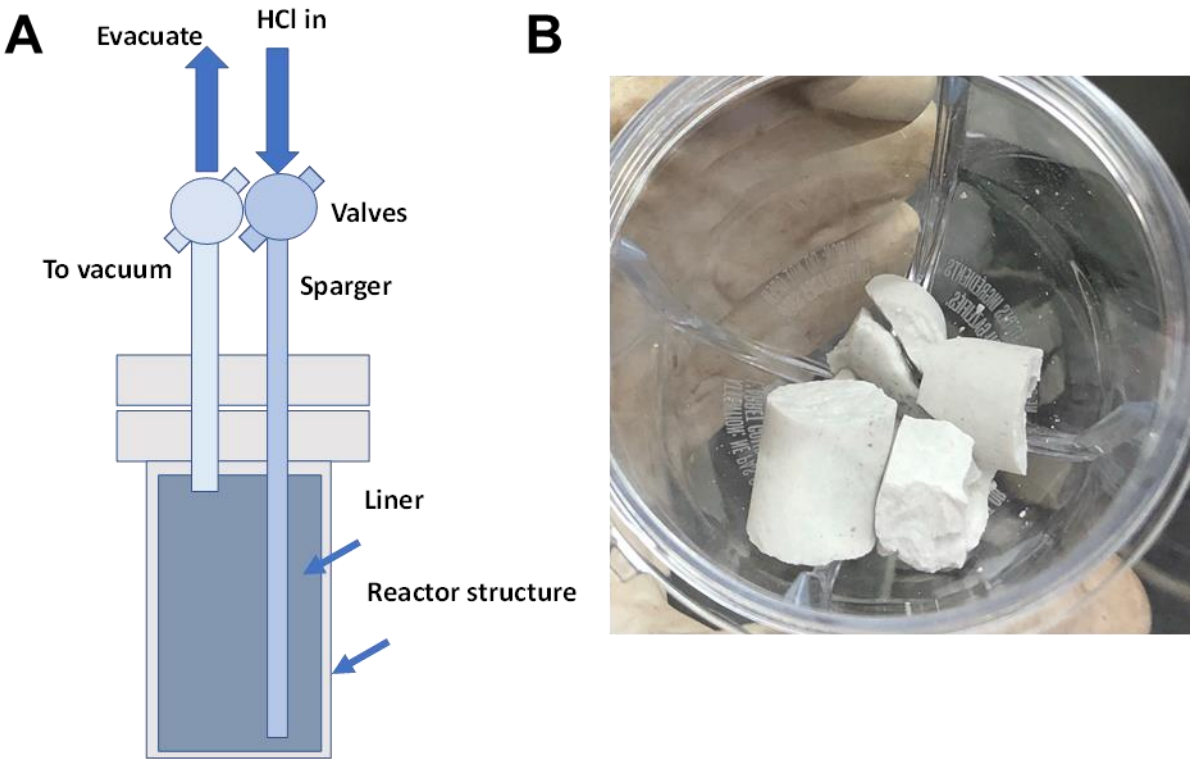

Figure 3-10. (a) Schematic of salt cleaning vessel and (b) the resulting cleaned LiCl-KCl salt.

The cleaned LiCl-KCl eutectic prepared by the method above, was melted at 575°C and U was added in the same method as described above with 4 additions of U(IV) (UCl_4 solid) followed by 2 additions of U(III) (UCl_3 solid). Overall, the melted cleaned eutectic showed a clear colorless melt, with fewer impurities than the unpurified commercial salt (Figure 3-11a). The resulting UV-vis spectra are shown in Figure 3-12. During the first 4 additions of U(IV) (labeled 1-4), both U(IV) bands at 455 and 670 nm increase. During this period, the U(III) at 563 nm remains near 0, indicating no U(III) present in the sample. The 480 nm band does increase during steps 1-4 because it overlaps with the shoulder of the 455 nm U(IV) band. During the subsequent two additions of U(III) (steps 5 and 6), there is an increase in the 563 nm U(III) band and a decrease in the 455 nm U(IV) band. This indicates that the U(III) at 480 nm is broadening the shoulder and resulting in a decrease in the 455 nm band. This can be seen in Figure 3-12b where the red-orange line for the second addition of U(III) has a broader shoulder in the 480 nm range. Photos were taken during this experiment and are shown in Figure 3-11. The green U(IV) can be seen after the additions of U(IV), but the red U(III) is not clearly discernable. This, along with the small U(III) UV-vis intensity, could indicate that the U(III) is reacting with impurities still present in the salt. This could also explain the increase in the U(IV) band at 670 nm after adding U(III) as it is oxidized to U(IV).

Figure 3-11. Photos of U in LiCl-KCl eutectic at 575°C (a) before the addition of U, (b) after 4 additions of U(IV), and (c) after two subsequent additions of U(III).

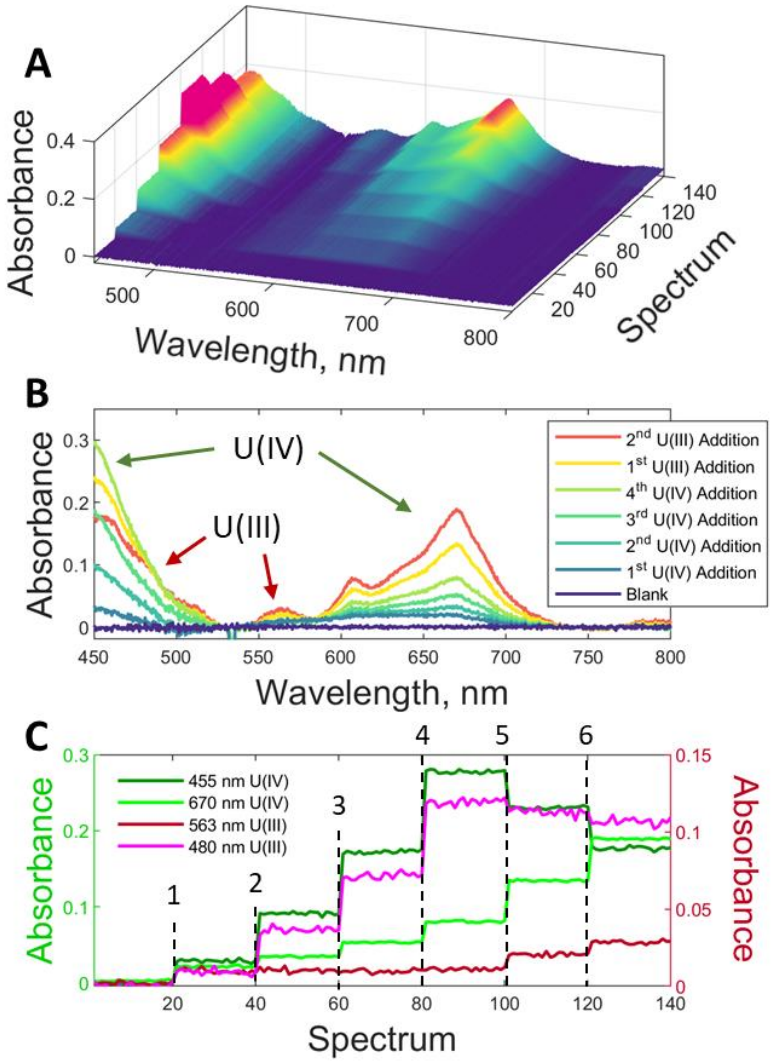

Figure 3-12. U behavior in LiCl-KCl eutectic at 575°C showing (a) UV-vis spectra collected after each of four additions of U(IV) (labeled 1-4) followed by two additions of U(III) (labeled 5, 6), (b) averaged spectra after each addition of U, and (c) the measured absorbance at the 455 and 670 nm peaks associated with U(IV) and the 563 and 480 nm U(III) peaks. The integration time was 2 sec.

4. CONCLUSIONS

This report highlights demonstrations on uranium, providing key U fingerprints under a variety of salt conditions in multiple oxidation states. Specifically, UV-vis and Raman spectroscopic analyses were utilized to measure uranium chloride salts in LiCl-KCl and NaCl-KCl-$MgCl_2$ eutectics. Chemical systems discussed here were generally simple (limited optical interferents of U) where planned future work will expand to more complex chemical systems.

Demonstrations were completed in a small-scale setup, enabling faster setup and requiring smaller quantities of analyte. The general system design has been used by the PNNL team previously, while the system used here includes modifications to allow for air sensitive measurements. Most importantly, the system was transitioned to an inert glove box enabling the interrogation of molten salts under controlled atmospheric conditions. The glovebox is maintained under Ar atmosphere O_2 <0.4 ppm and moisture <5 ppm; internal box pressure is maintained at 1.0 – 2.2 mbar positive from atmosphere. The custom furnace for handling molten samples sits inside of the glovebox, with several feedthroughs installed to accommodate connection to spectroscopic, temperature, and potentiostat instruments housed outside of the glovebox.

The ability to spectroscopically measure various oxidations states of uranium was demonstrated for U(IV) and U(VI) within the two distinct chloride-based eutectics. The first eutectic characterized was produced from high purity salts as received, the second was purified using HCl gas. In both systems calibration curves were generated through the sequential addition of U(IV) in the chemical form UCl_4. Following this, a chemical conversion of U(IV) to U(VI) was observed and fingerprints were captured during the heating period of this experiment. The quantitative conversion of the U(IV) to U(VI) was confirmed by the on-line monitoring and PLS modeling of the solution phase for the NaCl-KCl-$MgCl_2$ eutectic. Within this same eutectic the extinction coefficients for both U(IV) and U(VI) were confirmed to be consistent with literature for the UV-vis spectra of these species. In addition, the limits of detection for U(IV) (LOD 0.27 wt%; 18 mM) and U(VI) (LOD 0.17 wt%; 12 mM) were determined for UV-vis; and the limit of detection for U(VI) (LOD 0.013 wt%; 0.9 mM) was measured for Raman. Measurement of U(III) signatures was not achieved within the NaCl-KCl-$MgCl_2$ eutectic. Attempts to electrochemically convert U(IV) to U(III) resulted in the formation of black dendrites, likely indicating a chemical interferent in the salt was converting U(III) very quickly to solid precipitates.

Within the cleaned LiCl-KCl molten salt, U(III) and U(IV) signatures were measured by UV-vis. The UCl_3 and UCl_4 salts were dissolved in the purified LiCl-KCl eutectic at 575°C. The U salts were added in sequential additions of UCl_4 solid followed by additions of UCl_3 solid, with the resulting spectra showing the expected signatures for both U(III) and U(IV) solution species.

Overall, results indicate optical spectroscopy can be a valuable tool for characterizing U within molten salt environments. While observed limits of detection offer a good starting point, reducing these limits and uncertainties will be a goal moving forward. Furthermore, initial chemometric modeling on the NaCl-KCl-$MgCl_2$ eutectic data suggests robust U models can be effectively produced and used to quantify U. A major next step will be the inclusion of salts containing U and interfering analytes into the optical libraries to validate performance and accuracy under complex melt conditions.

5. ACKNOWLEDGEMENTS

This work was funded by the Department of Energy Office of Nuclear Energy's Advanced Reactor Safeguards Campaign. Pacific Northwest National Laboratory (PNNL) is operated by Battelle Memorial Institute for the DOE under contract DE-AC05-76RL01830.

6. REFERENCES

Bourgès, G., D. Lambertin, S. Rochefort, S. Delpech, and G. Picard. 2007. "Electrochemical studies on plutonium in molten salts." *Journal of Alloys and Compounds* **444-445**:404-09.

Bryan, S. A., T. G. Levitskaia, A. M. Johnsen, C. R. Orton, and J. M. Peterson. 2011. "Spectroscopic monitoring of spent nuclear fuel reprocessing streams: an evaluation of spent fuel solutions via Raman, visible, and near-infrared spectroscopy." *Radiochimica Acta* **99**(9):563-71.

Clark, P. V. 1965. *PHYSICAL PROPERTIES OF FUSED SALT MIXTURES. Data from Open Literature, 1907-1962*. SC-R-65-930(Vol.1) United States 10.2172/4613165 NTIS SNL English, Sandia Corp., Albuquerque, N. Mex.

Harris, D. C. 2007. *Quantitative chemical analysis*, 7 ed., W.H. Freeman and Co., New York, NY.

Lines, A. M., S. R. Adami, S. I. Sinkov, G. J. Lumetta, and S. A. Bryan. 2017. "Multivariate Analysis for Quantification of Plutonium(IV) in Nitric Acid Based on Absorption Spectra." *Analytical Chemistry* **89**(17):9354-59.

Lines, A. M., G. B. Hall, S. Asmussen, J. Allred, S. Sinkov, F. Heller, N. Gallagher, G. J. Lumetta, and S. A. Bryan. 2020a. "Sensor Fusion: Comprehensive Real-Time, On-Line Monitoring for Process Control via Visible, Near-Infrared, and Raman Spectroscopy." *ACS Sensors* **5**(8):2467-75.

Lines, A. M., G. B. Hall, S. I. Sinkov, T. Levitskaia, N. B. Gallagher, G. J. Lumetta, and S. A. Bryan. 2020b. "Overcoming oxidation state dependent spectral interferences: On-line monitoring of U(VI) reduction to U(IV) via Raman and UV-vis spectroscopy " *Ind. Eng. Chem. Res.* **59**:8894-901.

Lines, A. M., G. L. Nelson, A. J. Casella, J. M. Bello, S. B. Clark, and S. A. Bryan. 2018. "Multivariate Analysis To Quantify Species in the Presence of Direct Interferents: Micro-Raman Analysis of HNO_3 in Microfluidic Devices." *Analytical Chemistry* **90**(4):2548-54.

Lines, A. M., P. Tse, H. M. Felmy, J. M. Wilson, J. Shafer, K. M. Denslow, A. N. Still, C. King, and S. A. Bryan. 2019. "Online, Real-Time Analysis of Highly Complex Processing Streams: Quantification of Analytes in Hanford Tank Sample." *Industrial & Engineering Chemistry Research* **58**(47):21194-200.

Nagai, T., T. Fujii, O. Shirai, and H. Yamana. 2004. "Study on Redox Equilibrium of UO_2^{2+}/UO_2^{+} in Molten NaCl - 2 CsCl by UV-Vis Spectrophotometry." *Journal of Nuclear Science and Technology* **41**(6):690-95.

Nagai, T., A. Uehara, T. Fujii, O. Shirai, N. Sato, and H. Yamana. 2005. "Redox Equilibrium of U^{4+}/U^{3+} in Molten NaCl - 2 CsCl by UV-Vis Spectrophotometry and Cyclic Voltammetry." *Journal of Nuclear Science and Technology* **42**(12):1025-31.

Nagai, T., A. Uehara, T. Fujii, and H. Yamana. 2013. "Reduction behavior of UO_2^{2+} in molten LiCl – RbCl and LiCl – KCl eutectics by using tungsten." *Journal of Nuclear Materials* **439**(1):1-6.

Nelson, G. L., S. E. Asmussen, A. M. Lines, A. J. Casella, D. R. Bottenus, S. B. Clark, and S. A. Bryan. 2018. "Micro-Raman Technology to Interrogate Two-Phase Extraction on a Microfluidic Device." *Analytical Chemistry* **90**(14):8345-53.

Nelson, G. L., H. E. Lackey, J. M. Bello, H. M. Felmy, H. B. Bryan, F. Lamadie, S. A. Bryan, and A. M. Lines. 2021. "Enabling Microscale Processing: Combined Raman and Absorbance Spectroscopy for Microfluidic On-Line Monitoring." *Analytical Chemistry* **93**(3):1643-51.

Park, Y. J., S. E. Bae, Y. H. Cho, J. Y. Kim, and K. Song. 2011. "UV–vis absorption spectroscopic study for on-line monitoring of uranium concentration in LiCl–KCl eutectic salt." *Microchemical Journal* **99**(2):170-73.

Paviet, P., T. Hartmann, A. M. Lines, S. A. Bryan, H. M. Felmy, V.-A. Glezakou, M.-T. Nguyen, A. Medina, and S. D. Branch. 2020. *Corrosion of Molten Salt Containment Alloys - Fundamental Mechanisms for Corrosion Control and Monitoring*. PNNL-30379, Pacific Northwest National Laboratory, Richland, Washington.

Polovov, I. B., C. A. Sharrad, I. May, B. D. Vasin, V. A. Volkovich, and T. R. Griffiths. 2007. "Spectroelectrochemical Study of Uranium and Neptunium in LiCl-KCl Eutectic Melt." *ECS Transactions* **3**(35):503-11.

Polovov, I. B., V. A. Volkovich, J. M. Charnock, B. Kralj, R. G. Lewin, H. Kinoshita, I. May, and C. A. Sharrad. 2008. "In Situ Spectroscopy and Spectroelectrochemistry of Uranium in High-Temperature Alkali Chloride Molten Salts." *Inorganic Chemistry* **47**(17):7474-82.

Schroll, C. A., S. Chatterjee, T. Levitskaia, W. R. Heineman, and S. A. Bryan. 2016a. "Spectroelectrochemistry of $EuCl_3$ in Four Molten Salt Eutectics; 3 LiCl-NaCl, 3 LiCl-2 KCl, LiCl-RbCl, and 3 LiCl-2 CsCl; at 873 K." *Electroanalysis* **28**(9):2158-65.

Schroll, C. A., S. Chatterjee, T. G. Levitskaia, W. R. Heineman, and S. A. Bryan. 2017. "Electrochemistry of Europium(III) Chloride in 3 LiCl - NaCl, 3 LiCl-2 KCl, LiCl - RbCl, and 3 LiCl-2 CsCl Eutectics at Various Temperatures." *Journal of the Electrochemical Society* **164**(8):H5345-H52.

Schroll, C. A., S. Chatterjee, T. G. Levitskaia, W. R. Heineman, and S. A. Bryan. 2013. "Electrochemistry and Spectroelectrochemistry of Europium(III) Chloride in 3 LiCl - 2 KCl from 643 to 1123 K." *Analytical Chemistry* **85**(20):9924-31.

Schroll, C. A., A. M. Lines, W. R. Heineman, and S. A. Bryan. 2016b. "Absorption spectroscopy for the quantitative prediction of lanthanide concentrations in the 3 LiCl - 2 CsCl eutectic at 723 K." *Analytical Methods* **8**(43):7731-38.

Serp, J., R. J. M. Konings, R. Malmbeck, J. Rebizant, C. Scheppler, and J. P. Glatz. 2004. "Electrochemical behaviour of plutonium ion in LiCl–KCl eutectic melts." *Journal of Electroanalytical Chemistry* **561**:143-48.

Shirai, O., T. Iwai, Y. Suzuki, Y. Sakamura, and H. Tanaka. 1998. "Electrochemical behavior of actinide ions in LiCl–KCl eutectic melts." *Journal of Alloys and Compounds* **271-273**:685-88.

Tse, P., S. A. Bryan, N. P. Bessen, A. M. Lines, and J. C. Shafer. 2020. "Review of on-line and near real-time spectroscopic monitoring of processes relevant to nuclear material management." *Analytica Chimica Acta* **1107**:1-13.